Article:
Alizadeh, M, Asachi, M, Ghadiri, M orcid.org/0000-0003-0479-2845 et al. (2 more authors) (2018) A methodology for calibration of DEM input parameters in simulation of segregation of powder mixtures, a special focus on adhesion. Powder Technology, 339. pp. 789-800. ISSN 0032-5910

https://doi.org/10.1016/j.powtec.2018.08.028

A methodology for calibration of DEM input parameters in simulation of segregation of powder mixtures, a special focus on adhesion

Mohammadreza Alizadeh, Maryam Asachi, Mojtaba Ghadiri, Andrew Bayly, Ali Hassanpour*
School of Chemical and Process Engineering, University of Leeds, Leeds, UK.

*Corresponding author:
Tel: +44(0)113 343 2405
A.Hassanpour@leeds.ac.uk

Abstract
Conducting a numerical simulation for cohesive granular mixtures that is well comparable with experiments has always been a challenge. In this study, a systematic methodology is proposed for increasing the fidelity of Discrete Element Method (DEM) simulations of cohesive powder mixtures. Segregation of granules during heap formation of a ternary powder mixture is simulated as a proof of concept. The mixture contains three model particles, one of which is an enzyme placebo granule (EP), in order to simulate the segregation of the actual enzyme granules used in detergent formulations. These granules are at a low content level ($\sim$2 wt%) and are highly prone to segregation. In this study the segregation tendency of the EP granules is mitigated by coating them with Polyethylene Glycol 400 (PEG 400). The resulting adhesion is expressed in terms of equivalent interfacial energy for the DEM numerical simulations, and is tuned by careful calibration using the concept of the angle of repose. The Cohesion number is used to scale material stiffness or changing the particle size for faster simulation. The particles shapes in DEM are modelled as clumped spheres based on the X-ray tomograms of the real particles. The rest of the DEM input parameters are also selected and tuned based on the particles physical and mechanical properties.

Considerable reduction in segregation tendency of the low level ingredient granules is observed as a result of coating its surfaces by PEG400. Following the proposed calibration strategy, the DEM simulations have predicted the experimental trends closely and a reasonable agreement is achieved. It is observed that using the Cohesion number for scaling the interfacial energy can significantly reduce the number of calibration trials.

Key words: Segregation; Discrete Element Method; polydisperse system; flowability; coating; heap formation; Cohesion number

1 Introduction

DEM modelling of powder and granular processes has become a popular and useful complementary tool for analysing the mechanisms of particles interaction and predicting their behaviour in experimental and industrial processes. DEM is a powerful tool for elucidating the underlying mechanisms of granular phenomena in various processes and products. Nevertheless, it is a very computationally expensive method for modelling a real granular process, as the number of particles in practice is excessive. This shortcoming is partially compensated by scaling-up the particle size, scaling-down the materials stiffness, and/or using simplified representation of particles (coarse-graining) in DEM simulations [1, 2]. This helps modelling the process by a smaller number of computational elements and larger time steps than for the real system, both of which significantly reduce the computational cost.

Utilising a scaled DEM input parameter adventitiously may produce misleading results. The scaling issue becomes more critical when the materials under study are cohesive, where depending on the utilised contact model, scaling the particle size and stiffness changes the inter-particulate attractive forces considerably [2, 3]. This change in micromechanics of the granular system leads to unrealistic bulk behaviours. Despite the ever rising popularity of the DEM simulations, a comprehensive approach for scaling and calibration of the DEM input parameters according to the real experimental values is still missing in the literature.

In this study, a systematic methodology is proposed for selection and calibration of the DEM input parameters with a particular focus on scaling the particles interfacial energy according to a rule taking account of size, stiffness, shape, and density. As a proof of concept, this methodology is applied to a case of segregation of particles during a heap formation process in a confined box.

There are various ways of controlling the segregation, including applying modifications to equipment geometry, changing the process operating conditions, balancing the effects of particles size and density, and/or manipulating their surface condition [4-7]. Focusing on the latter, it has a significant impact on inducing or reducing segregation mainly by influencing the flowability and mobility of particles [8]. Coating particles is a common and relatively easy method of manipulating their surface condition, by which the powder mixture can be transformed from cohesive to free flowing mode and vice versa [9-11]. Dry coating is commonly used in industry to increase the flowability of sticky particles [9, 10, 12], whereas adding binders (mostly in liquid form) has the opposite effect. It reduces the particle motion and potentially helps in maintaining mixture homogeneity for a longer time [11, 13]. However, any improvement in homogeneity of a mixture by liquid addition comes at the cost of reduced flowability; potentially causing handling problems and imposing extra costs [14-17]. So an optimisation is needed to provide a balance between the tendencies of segregation and flowability, and this can be executed by numerical simulation using DEM.

To mimic the effect of particle adhesion in DEM modelling, adhesive contact models are used, e.g. elastic adhesive models [21, 22] for perfectly elastic contacts and elasto-plastic adhesive models [23, 24] for contacts which experience plastic deformation as well. A perfectly elastic adhesive contact model, like the JKR (Johnson-Kendall-Roberts) [21], can be used in many cases provided that the particles bear relatively low stresses [25]. A systematic methodology to predict and calibrate the interfacial energy for DEM modelling is needed. This is done by matching the experimental repose angle with that predicted by DEM simulation, whilst tuning the surface energy.

As a proof of concept, the effect of coating on segregation tendency of a low level ingredient in a ternary powder mixture during heap formation is modelled. Heap formation is affected by the particles physical and mechanical properties such as size, density, shape, and surface conditions such as adhesion and friction. So where possible, some of the properties are measured directly and the rest are inferred by calibration using DEM simulations. In the experiments, the minor component is coated by PEG 400 to manipulate its stickiness and is mixed with the rest of species. The homogeneity of particle number distribution in the heap is assessed for the uncoated and coated granules and the results are compared with the experimental data. The underlying mechanisms of particle segregation before and after coating are analysed using DEM and reported here.

2 Methodology

2.1 Geometry

The geometry of the test box used in this study is shown in Fig. 1. In the experiments, the box walls are transparent made from Perspex and the box frame is metallic. The powders are mixed manually and poured into the funnel from which the mixture is introduced into the box to form the heap. The procedure of doing the experiment is further described by Asachi et al. [7]. This process is simulated by DEM with the same geometrical specifications as of the experiment. The physical parameters are measured where possible and used in DEM as detailed below.

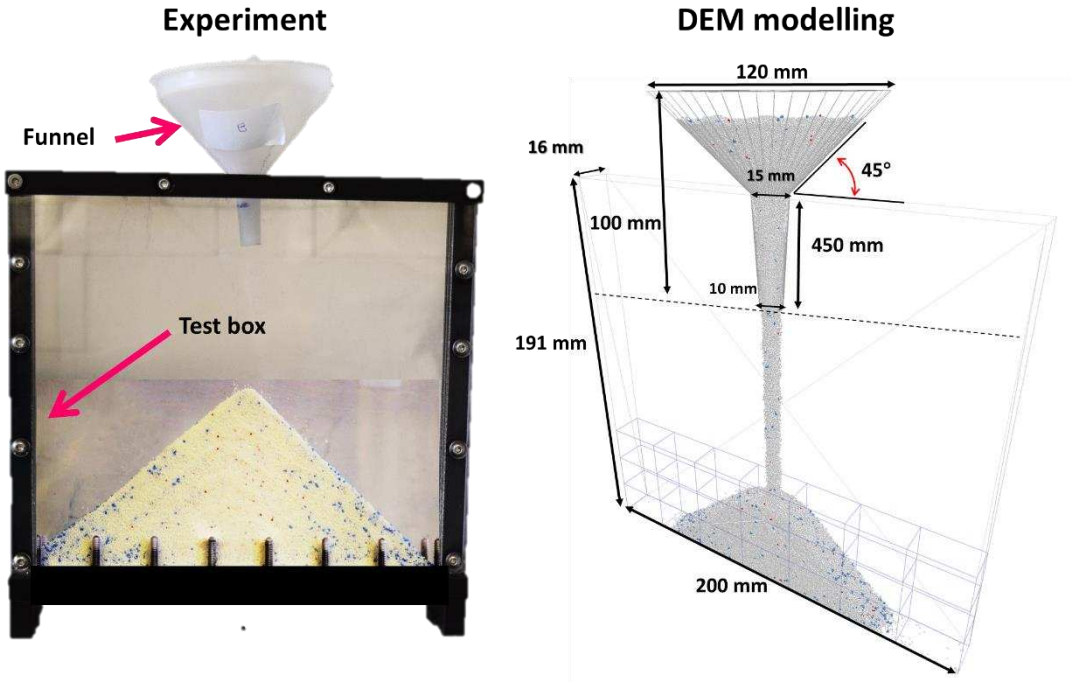

Fig. 1 : Image of the geometry of the test box used in the experiment and modelling. (The bottom of the image of the heap test box shows a number of screws holding the front transparent wall and are not intruding the powder bed)

2.2 Computational methodology

EDEM 2.7.1 software, provided by DEM Solutions, Edinburgh, UK, is used to model the heap formation process. The models used for particle interactions are Hertz-Mindlin [21, 26, 27] for elastic deformation and frictional traction and JKR [21] for adhesion. The particles used in this study are relatively large and soft and do not experience high stresses, therefore the JKR theory is valid for this case according to the Tabor criterion [25]. The details of these models are available elsewhere [28, 29]. Before coating the EP granules, the contact adhesive interactions are not dominant and hence negligible compared to the gravitational force (high Bond number [30]). Therefore for simulation of the mixture with no coated particles, the JKR model is switched off and the contact model is reduced to Hertz-Mindlin. For the coated EP granules, the appropriate interfacial energy values are inferred by comparing the simulation results with those from experiments, as will be detailed in section 2.5 [31]. The particle shape has previously been characterised by X-ray Tomography (XRT). It is approximated using the clumped sphere

approach [32]. Their general shape, aspect ratios in different directions, envelope volume, and the relative position of the centre of mass are optimised to be as close as possible to the original real shape as detailed below.

2.3 Particles physical and mechanical properties

The spray-dried detergent powder (termed Blown Powder, abbreviated to BP) and TetraAcetylEthyleneDiamine (TAED) particles used in this study are the main ingredients of conventional home washing powders. In some detergent formulations active enzyme granules are also used. For safety reasons, placebo granules are used instead in this study, abbreviated as EP. Typical shapes of granules used are shown in Fig. 2.

The same materials and conditions as of Asachi et al.'s experiments are used in this work [7]. The particles are sieved and their size is selected based on the sieve cut corresponding to the mode of their size distribution. The particle properties used in the simulations are given in Table 1. The method of characterisation of these properties is fully described by Alizadeh et al. [33]. The three components are mixed manually, using mass fractions that are representative of the formulation of washing powders, and introduced into the test box to form the heap (Fig. 1). It should be noted that only the EP granules are made sticky in this study, as it is more prone to segregation compared to other species. It is also highly active and its segregation has potential health hazards. For the coefficients of sliding friction (CoF) and rolling friction (CoR) of the BP and TAED particles, the same values as those calibrated and used in [33] are utilised here. For the coated EP granules, a special methodology is utilised for calibration of their interfacial energy which will be described in further detail later in the following.

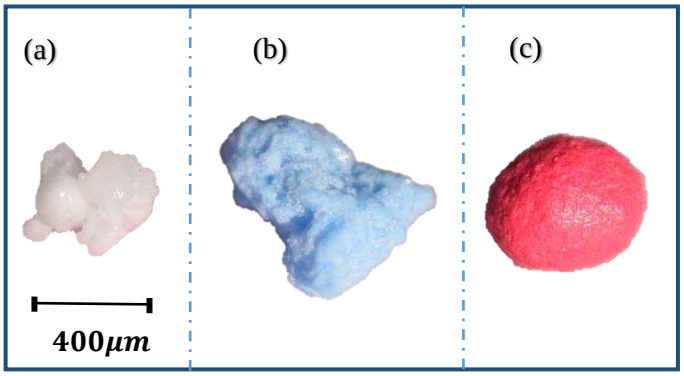

Fig. 2: Typical shapes and colours of (a) BP, (b) TAED, and (c) EP granules shown by optical images.

Table 1. Specifications of the modelling and the material properties.

Material type	BP	TAED	EP	Perspex
Size (μm)	425-500	850-1000	600-700	
Particles number	633,597	4667	1401	
Total mass (g)	28.53	1.71	0.61	
Mass generation rate ($g.s^{-1}$)	18.5	1.1	0.4	
Weight Percentage	92.0	6.0	2.0	
Particle shape	5-sphere	5-sphere	1, 2, 3-sphere	Wall
Repose angle (uncoated) (°)	40.0	36.0	31.0	
Shear modulus (MPa)	100	100	100	1000
Density ($kg.m^{-3}$)	780	850	2320	1180
Coefficient of rolling friction	0.10	0.01	0.05	0.01
Poisson's ratio	0.25	0.25	0.25	0.25
CoF (BP-particle)	0.62	0.69	0.70	0.42
CoF (TAED-particle)	0.69	0.75	0.75	0.36
CoF (Placebo-particle)	0.70	0.75	0.75	0.75
CoR (BP-particle)	0.20	0.30	0.20	0.28
CoR (TAED-particle)	0.30	0.32	0.20	0.32
CoR (Placebo-particle)	0.20	0.20	0.10	0.20

2.4 Particle shape

The particle shapes of the components are different due to differences in processes by which they are manufactured. To account for particle shape, particles are randomly selected from each component and scanned by the XRT technique using a Nanotom X-ray computed tomography machine (Phoenix, Wunstorf, Germany)). The scans are then analysed using an image analysis software, Avizo 3D, and the particles shapes are reconstructed and exported as mesh files (.stl) to the Automatic Sphere-clump Generator (ASG) software company (Cogency, Cape Town, South Africa) [34]. Different number of spheres can be used to mimic a real particle shape, where a larger number of constituting spheres clumped together provide a better representation of the real particle shape. This, however, requires more computations in DEM due to the increase in the computational elements. To find an optimum number of spheres for each clump, whereby the least computational effort is required for achieving an accurate result, an optimisation study is carried out by comparing the simulated angle of repose of the clumped spheres with that of the experiments. The selected particle shapes and their corresponding optimum clumped spheres are presented in Fig. 3. In the present study, BP and TAED particles are modelled only by one shape each, which is able to mimic the experimental angle of repose. For the EP granules both spherical shape and three spheres clumped together approximating prolate spheroid shape are used. The details of the shape calibration method are further described in our previous work [33].

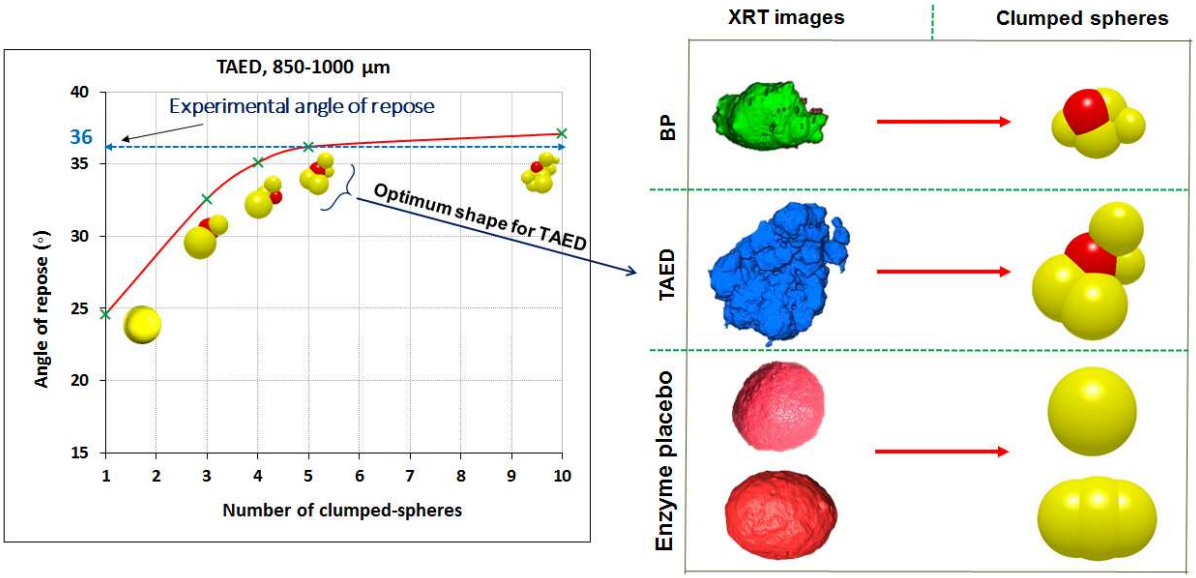

Fig. 3: Particle shape optimisation based on XRT images of the particles and experimental angle of repose [33]. For each species, the minimum number of spheres by which the clumped sphere can accurately mimic the experimental repose angle is selected and presented.

2.5 Modelling the adhesion

2.5.1 Background

Coating the surfaces of the EP granules with a small quantity of PEG 400 makes the surfaces sticky without developing capillary bridges. In this case the adhesive interfacial energy is approximated by the JKR model [21] for which an appropriate value is needed. To account for viscous dissipation, low restitution coefficients are selected. This is done by calibrating the interfacial energy so that the repose angles of experimental work and simulations match. However, the use of the actual surface energy and contact stiffness in DEM simulations gives rise to long simulation times. Therefore a robust criterion in needed to scale the surface energy and stiffness. Using the Bond number [36], which is the ratio of the gravitational force and the adhesive force, is one of the few ways of scaling. However, this number does not include Young's modulus to account for deformation. Another method proposed by Thakur et al. [37], scales the surface energy with the square of particle radius. This scaling rule is obtained by exploring and comparing linear, quadratic, and cubic scaling of adhesive force with particles radius for special

cases of confined and unconfined uni-axial loading and unloading process. Another method is to compare the Cohesion energy (energy needed to detach two particles after coming into contact) with the gravitational potential energy of the particles. This was first proposed by Behjani et al. [3] as the Cohesion number which is expressed in Equation (1),

$$\mathrm{Coh} = \frac{1}{\rho g}\left(\frac{\Gamma^5}{E^{*2}R^{*8}}\right)^{1/3} \tag{1}$$

where g, ρ, and Γ are gravitational acceleration, envelope density, and interfacial energy of the particles respectively. R^* and E^* are the reduced radius and Young's modulus of elasticity of the spheres, respectively:

$$R^* = \left(\frac{1}{R_1} + \frac{1}{R_2}\right)^{-1} \tag{2}$$

$$E^* = \left(\frac{1-{\nu_1}^2}{E_1} + \frac{1-{\nu_2}^2}{E_2}\right)^{-1} \tag{3}$$

where R_1 and R_2 are the radii of the spheres, E_1 and E_2 are their Young's moduli, and ν_1 and ν_2 are their Poisson's ratios.

The Cohesion number is a useful scaling method for the DEM simulations for which Young's modulus is selected smaller than the real value in order to increase the computational speed. Recently, a rigorous analysis of contact stiffness reduction for adhesive contacts to speed up DEM calculations shows the same functional form [2].

Table 2. The physical and mechanical properties of EP granules and PEG400.

Material	Property	Value
EP	Sieve-cut Size (μm)	600-700
	Density ($\mathrm{kg.m^{-3}}$)	2320
	Young's modulus for placebo (GPa) [39]	1.6
	Poisson's ratio	0.25

	Interfacial energy in DEM ($\mathrm{J.m^{-2}}$)	0.0 - 0.350
PEG 400	Surface energy in experiment ($\mathrm{J.m^{-2}}$) [40, 41]	0.043

2.5.2 Evaluation of the EP granules interfacial energy

The process of evaluation of the particles interfacial energies to be used in DEM modelling is presented as a flow chart in Fig. 4. For the coated EP granules the initial value of the surface energy is based on the surface tension of the PEG 400. Then the angle of repose is used as the criterion for tuning the surface energy. To do so, the process of heap formation for the EP granules with each level of coating is carried out experimentally and its corresponding angle of repose is measured. It should be noted that for lower levels of coating (less than 2.5 wt% of PEG) the heap edges are sharp straight lines and the angle of repose is measured accurately; while for the higher levels of coating, due to the fluctuations on the heap surface, the angle of repose is measured considering the average angle of the heap profile. For this, the heap is divided into right and left sections as displayed in Fig. 5. For each section, the horizontal distance between two points on the heap surface which correspond to 10% to 90% of the heap height is measured as shown in Fig. 5, from which the repose angle is calculated. The final value for the repose angle is the average of the values measured for the left and the right sections. The angle of repose test is repeated five times for each level of coating and the average value is reported in Fig. 6, where the error bars show the variations in the repose angle at each case. Clearly, the error band depends on how sticky the granules are.

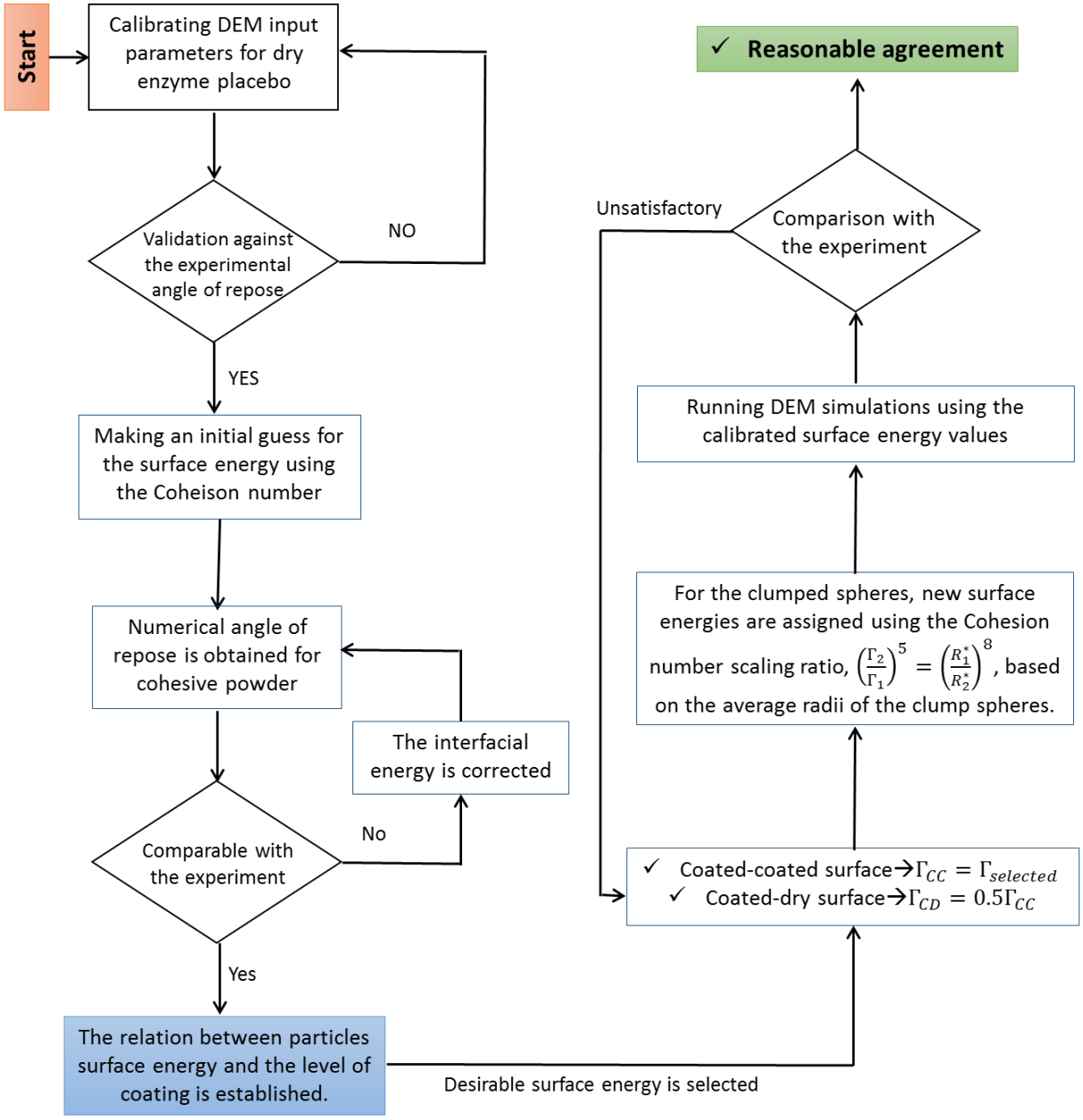

Fig. 4. Schematic of the interfacial energy calibration methodology in a flow chart.

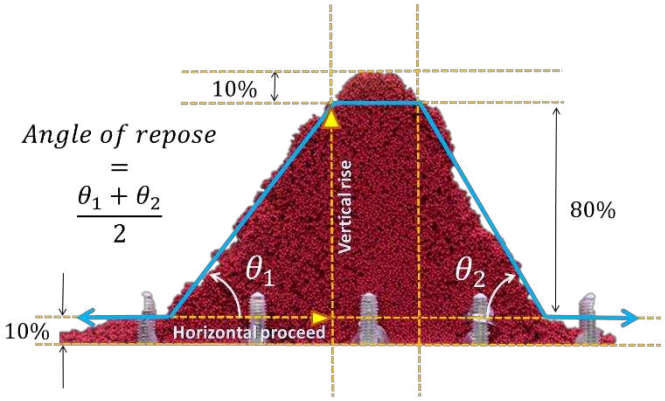

Fig. 5. The method of determining the angle of repose of cohesive powders.

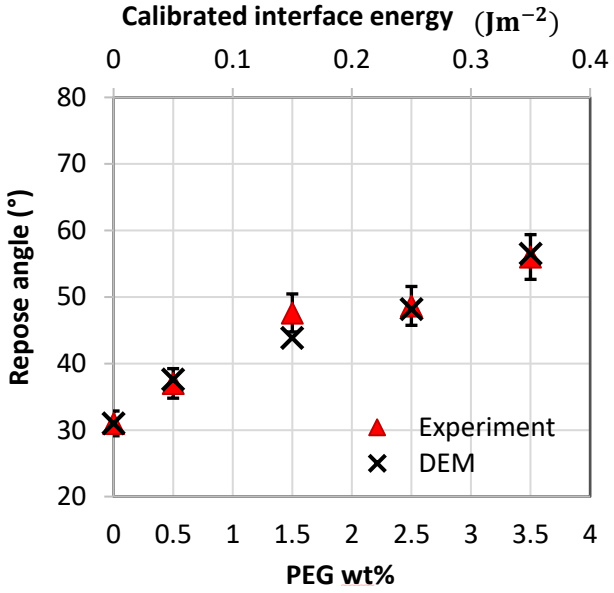

Fig. 6 **:** Calibration of the EP granules interfacial energy based on level of coating using the angle of repose approach.

For the dry granules, the interfacial energy is set to zero in the DEM simulation, giving a repose angle which matches nicely with that from the experiment, i.e. 31.0°. For DEM simulation of the coated granules, the initial value of the interfacial energy is based on the surface tension of PEG 400, and scaled using the Cohesion number for a lower value of Young's modulus than that of real EP granules. The surface energy of the coating material, γ_{PEG} is $0.043\,\mathrm{J.m^{-2}}$ [40, 41]). Therefore, the interfacial energy of the EP granules is taken as $\Gamma_{EP} \cong 2\gamma_{PEG} = 0.086\,\mathrm{J.m^{-2}}$ [42].

Using this value in combination with the particles density, radius, and modulus of elasticity, listed in Table 2, the Cohesion number of the coated particles in the experiments is found to be 1.6×10^{-3}. The value of Young's modulus used in the simulations is taken as nearly one order of magnitude smaller than the real value (i.e. $\sim 0.25\ GPa$ compared to $1.6\ GPa$) to speed up the computations. Now keeping the value of the Cohesion number the same as of the experimental one, the equivalent interfacial energy for the lower Young's modulus is calculated as $0.046\ \mathrm{J.m^{-2}}$. Using this initial value for the simulation of heap formation gives an angle of repose of 37.6°. It turns out that this angle of repose matches that of the experimental case with 0.5 wt% PEG. Further calibrations are carried out to tune the interfacial energy in DEM so that the simulated angle of repose matches with the experimental one for other levels of coating (1.5-3.5 wt% of PEG). The equivalent interfacial energy for different mass fractions of coating material is displayed in Fig. 6. In addition, a visual comparison between the heaps from the experiment and DEM modelling is made in Fig. 7, where a good match prevails.

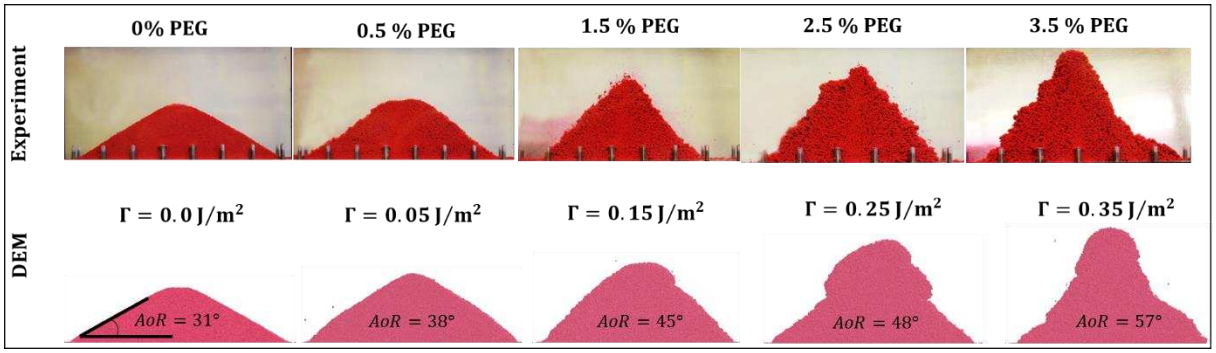

Fig. 7. The angle of repose of EP granules obtained from DEM and experiment for different levels of coating.

2.5.3 Setting the interfacial energy of dissimilar species

As mentioned before, the current study is based on the experimental study of Asachi et al.'s [7]. Therefore the same materials and conditions are used here. As reported previously [7], the lowest segregation index was observed when the EP granules were coated by 2.5 wt% of PEG.

Therefore we focus on this coating level and analyse three scenarios in the present study, i.e. the uncoated, optimally coated, and excessively coated, the latter producing very sticky EP granules. The equivalent interfacial energy for the EP contacts in the DEM modelling is found to be 0.250 Jm^{-2} for 2.5% PEG as shown in Fig. 6. To find the interfacial energy of the EP-BP and EP-TAED contacts, some assumptions and calculations are necessary. When the coated EP granules are mixed with the other particles, the adhesive surfaces of the EP granules make contact with the dry surfaces of the BP/TAED particles. Since the relationship between the coating level in experiment and the interfacial energy in modelling is almost linear, as inferred from Fig. 6, it is assumed that the interfacial energy of the contact of dry-adhesive surfaces is half of that of the case where both surface are adhesive, based on JKR model. The value obtained from this method shows the interfacial energy (Γ_1) of two spheres with equal sizes (R_1^*). However, the sizes of the BP and TAED particles are different from the EP granules. In this case the equivalent volume radii of the BP and TAED particles are used to find R_2^* from Equation (2) for EP-BP and EP-TAED contacts. The relationship between the interfacial energy and the particle size is derived from the Cohesion number and expressed by Equation (4),

$$\Gamma_2 = \Gamma_1 \left(\frac{R_1^*}{R_2^*}\right)^{\frac{8}{5}} \tag{4}$$

The equivalent interfacial energy values of the EP-BP and EP-TAED (Γ_2) are predicted to be 0.037 and 0.060 Jm^{-2}, respectively, and are used in the simulations of the segregation index as described below.

2.6 Segregation index

There are various segregation indices, most of which are based on variance [43-49]. One of the indices used widely to describe the extent of segregation is the coefficient of variation [49-51] (CoV), which is the ratio of the standard deviation to the mean value. In the present study, the experimental method for determining the segregation index is based on image analysis of the

front/back of a pseudo-2D heap. The three components of the formulation have different colours, as shown in Fig. 3, making it possible to identify the particles of each component. This gives a 2-dimensional information about the homogeneity of the mixture. To do so, firstly an image is taken from the front/back view of the heap. It is then divided into 21 bins (Fig. 8), where the bin size is defined based on the scale of scrutiny, in the case here a scoop of washing powder. To have a 3-dimensional overview of the homogeneity of the mixture, DEM simulations are carried out and the mass concentrations of EP granules in the bins are calculated based on the population of each component. The coefficient of variation of these concentrations, $\mathrm{CoV_i}$, is then calculated by Equation (5) to show the segregation tendency of the species,

$$\mathrm{CoV_i} = \frac{\sigma_\mathrm{i}}{\mu_\mathrm{i}} \tag{5}$$

where σ_i is the standard deviation of EP granule concentrations (or mass fractions for 3D analysis) of species i and μ_i is their mean value [33].

Considering the population at each bin the probability of taking a certain component during the sampling is related to the concentration of that component [52]. This becomes more important when the component under investigation is a minor one, and it is the case here for the EP granules. To have a reliable judgment about the mixture quality, the CoV of a randomly mixed system is also calculated using Equation (5). The standard deviation for this case is calculated from Equation (6) [49, 53],

$$\sigma_R = \sqrt{\frac{\mathrm{P}(1-\mathrm{P})}{N}} \tag{6}$$

where P accounts for the probability of species present in the bin and N is the total number of particles in each bin when the particles are monosized. The random standard deviation depends on the number of similar particles that can be fitted in a sample bin; i.e. the particles should be similar in size and shape. Therefore, the total number of EP granules that can be fitted in a single bin for a random mixture, N, is approximated based on the volume of the bin, volume of an EP granule, and loose packing fraction for solid spheres, 0.6 [54]. The bins located in the corners

and edges of the heap are partially empty and their equivalent N values are smaller than that of a full bin and are taken into account as well. After finding the value of N for each bin, a random generator number is used in the Excel software by which a mass fraction is allocated to each bin based on the mean value of the mass fractions and the standard deviation obtained from Equation (6). The CoV of the mass fractions is then calculated and this process is repeated for 100 times to find a reliable average value (with high certainty) for the CoV of the random mixture ($\mathrm{CoV_r}$). The ratio of the CoV of the simulated mixture ($\mathrm{CoV_m}$) over the CoV of the random mixture ($\mathrm{CoV_r}$) is the normalised segregation index given by Equation (7), which is essentially the same as the index proposed by Poole et al. [55],

$$\mathrm{S_n} = \frac{\mathrm{CoV_m}}{\mathrm{CoV_r}} \tag{7}$$

The $\mathrm{S_n}$ values smaller or equal to one indicate a well-mixed mixture and the values over one show a segregated system.

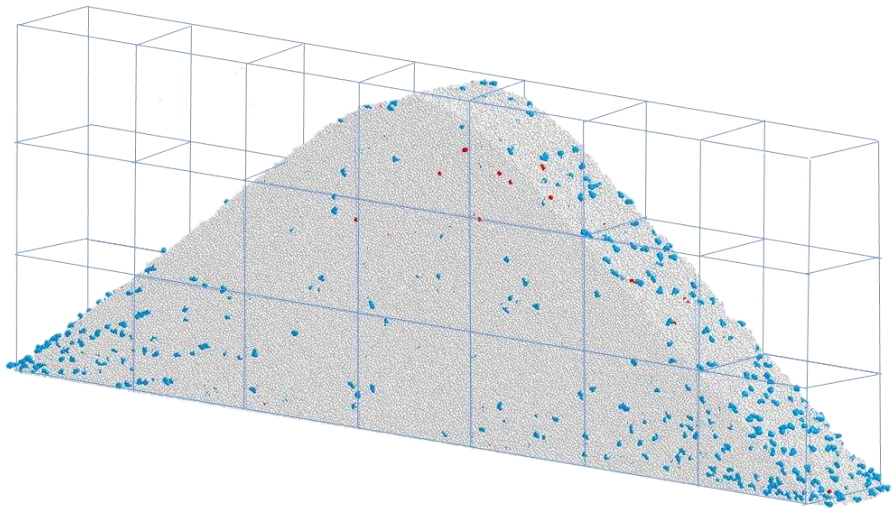

Fig. 8. Discretisation of the heap into bins for calculating the segregation index.

The image analysis technique described above is used for both experiments and DEM simulations to compare and validate the results. This is only applicable for the surface of the heap from which the image is taken; however in DEM, it is possible to observe the particles distribution

across the depth of the heap. In this regards the heap is discretised three-dimensionally into a number of bins in which the mass concentrations of the species are calculated and their CoV for the entire heap is then obtained. The same segregation index used for image analysis is applied here for finding the CoV of mass concentrations of species in DEM.

2.7 Mixtures flowability

There are various ways to assess how easily the bulk of powder flows. In this study the flow behaviour of the powder mixtures is assessed using the angle of repose and the Jenike flow index [56]. In the first approach the values of the angle of repose of the bulk of powder, before and after coating are measured and compared. In the second approach, i.e. the Jenike flow index, the Schulze ring shear cell device is used to measure bulk cohesion, represented by the unconfined yield stress, under different levels of consolidation stress. The Jenike flow index ($\mathrm{ff_C}$) is the ratio of the maximum principal consolidation stress σ_1 to the unconfined yield stress σ_c as described in [57]; Equation (8) shows the Jenike flow index.

$$\mathrm{ff_C} = \frac{\sigma_1}{\sigma_c} \tag{8}$$

The flow regimes of the bulk of powders can then be classified with regards to the value of $\mathrm{ff_C}$ as provided in Table 3.

Table 3: Classification of the flow regimes based on the Jenike flow function [58].

$\mathrm{ff_C}$ value	Flow regime
$\mathrm{ff_C} < 1$	Not flowing
$1 \leq \mathrm{ff_C} < 2$	Very cohesive
$2 \leq \mathrm{ff_C} < 4$	Cohesive
$4 \leq \mathrm{ff_C} < 10$	Easy flowing
$\mathrm{ff_C} < 10$	Free flowing

2.8 Particle generation in DEM

Once all the particles are characterised and the interfacial energy of the coated placebo granules is calibrated, particles are generated and introduced into the test box (Fig. 1) to form the heap. The three particle types are generated simultaneously at a constant rate (dynamic factory) according to the mass ratio reported in Table 1. Also, the particles are randomly generated in the factory and spatially distributed and let fall down into the funnel to make sure that the mixture is initially homogeneous. The results are given in the following section.

3 Results

3.1 Segregation on the side walls (2D analysis)

Two sets of simulation are carried out using the coated and uncoated EP granules. In the first test, particles are uncoated and free flowing, so their interfacial energy is set equal to zero. In this situation, although EP granules (red particles) are rounded and relatively larger than BP, they tend to accumulate in the central area of the heap due to their higher density, which is observable from the front view of the experimental heap (Fig. 9 (A)) and DEM simulation (Fig. 9 (B)). In contrast, the corners of the heap lack EP granules; this is clearer when looking at the exaggerated indexed images from the DEM analysis shown in Fig. 9 (C), where the EP granules are visually enlarged by image formatting. On the other hand, having the EP granules coated has caused them to be well distributed in the heap front face and even in the heap corners. It is observed that the DEM results are in agreement with the experimental ones, and their comparison is better visualised by the indexed images of the front side.

The CoV of the pixel concentrations of placebo granules is calculated for the system before and after coating and a comparison is given in Fig. 10. A reasonable match between the results of the experiments and simulations is observed with approximately 10% variations. It is also observed that coating has mitigated the segregation extent significantly, where CoV is reduced by at least 40%.

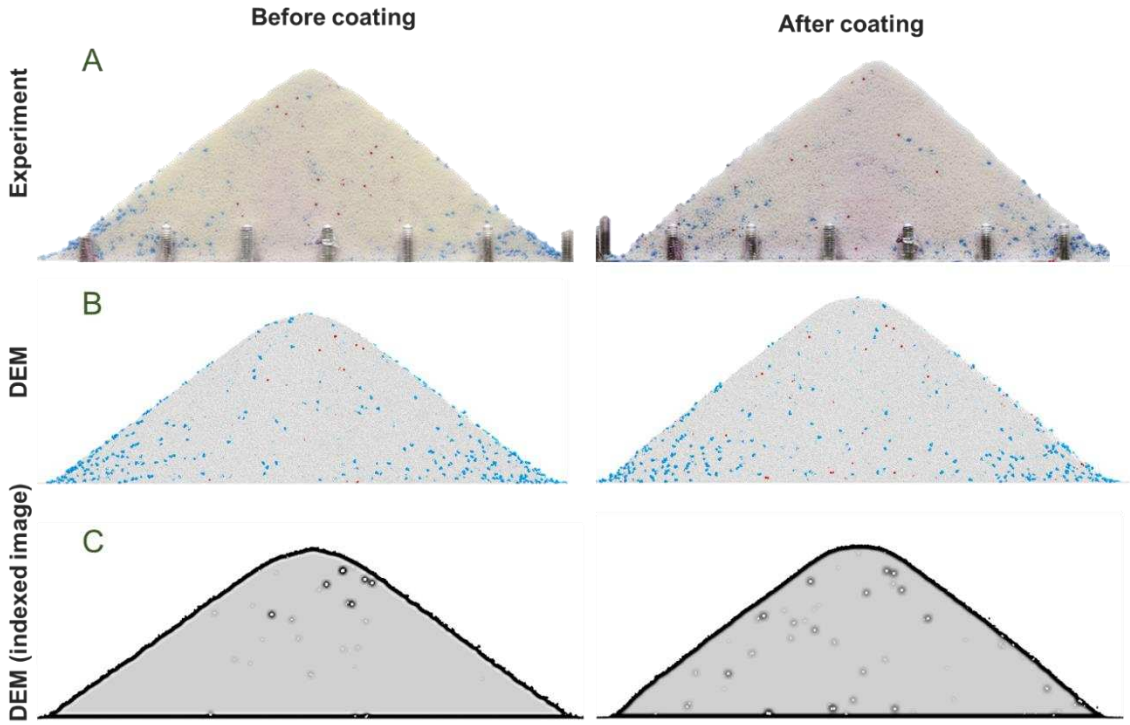

Fig. 9 **:** Heap formation of a ternary mixture of BP (white), TAED (blue), and EP (red) granules in experiment and DEM simulations . The mixture composition for BP, TAED, and enzyme granules is 50:3:1 by mass ratio. The enzyme granules are shown by white colour and black outline in the indexed image (C) and enlarged to show their number population in the image.

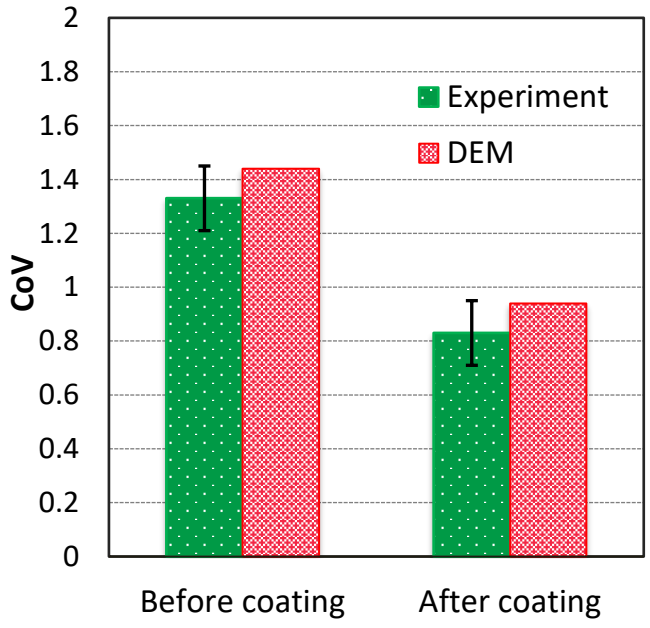

Fig. 10. The CoV of the EP granules before and after coating obtained by image analysis.

3.2 Particle distribution inside the heap (3D analysis)

The spatial distribution of placebo granules through the depth of the heap is displayed in Fig. 11. In each case, the heap thickness is divided into eight layers (2 mm thick) and the spatial distribution of the EP granules is presented for layers 1, 3, 6, and 8. It is clear that the segregation extent increases from the middle to the back and front sides of the heap before coating. After coating, the distribution patterns become more uniform and there is less variation in placebo distribution through the depth of the heap. This can also be observed from Fig. 12, where the CoV of the EP granules at different depth layers of the heap is provided. Clearly, coating the particles has led to low variations in CoV through the depth of the heap and the average value of the CoV for the entire heap has also decreased significantly after coating. It is also evident that for both coated and uncoated systems the middle layers (layer numbers 3 to 6) have lower CoV values. This indicates that the visible wall segregation is not well representative of the segregation of the entire mixture for the freely flowing uncoated system.

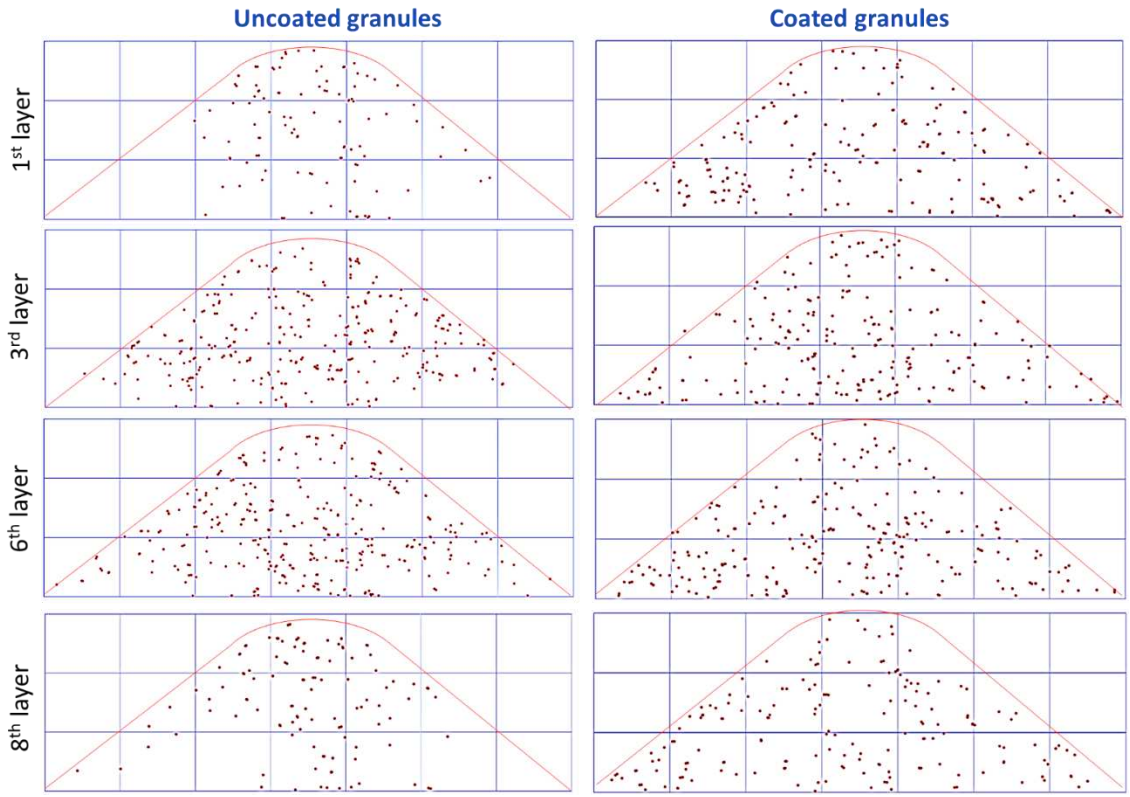

Fig. 11 : The distribution patterns of the EP granules within the selected layers across the depth of the heap (DEM simulations). The other species have been removed from the images and the EP granules have been enlarged by 100% to be easier observable.

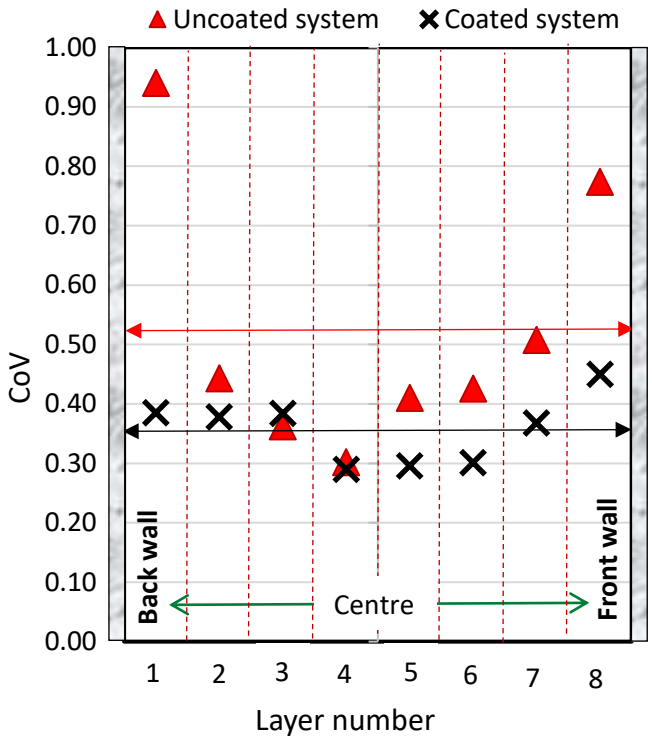

Fig. 12. The CoV of the EP granules at different depth layers from the central layer of the heap, obtained from particles mass fractions (DEM simulations).

The CoV of placebo granules for a randomly mixed system is calculated as described before. The values of $\mathrm{CoV_r}$ for the whole mixture and the front layer are equal to 0.21 and 0.50, respectively. Using these values the segregation index, S_n, on the front face (2D analysis) as well as for the entire heap (3D analysis) is calculated and presented in Fig. 13. All the analyses show that S_n is greater for the uncoated EP granules than that of the coated ones, as the segregation index drops to less than one after coating for the case of the whole heap. It is also clear that the segregation indices on the front and back faces are larger than that of the whole mixture. Coating has caused the segregation index to decrease by more than 70% in total and well over that locally

near the side walls. Although the segregation indices of the front/back faces (2-D analysis) are not comparable with the whole mixture (3-D analysis) due to packing differences, their decrease due to the coating shows similar patterns in both approaches.

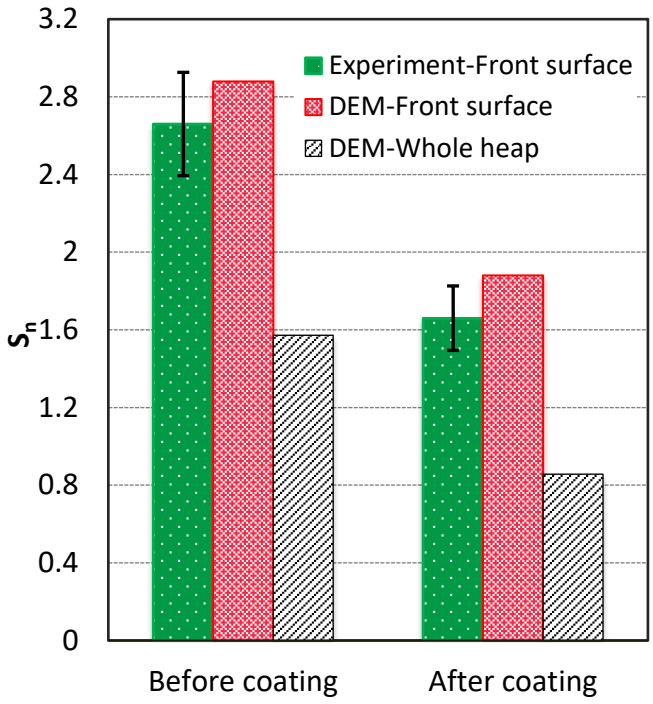

Fig. 13. The segregation index of the EP granules obtained by image analysis (2D analysis) and particles mass fraction in the heap (3D analysis).

3.3 Effect of coating on mixture flowability

The images of the simulated heaps, showing the particles spatial distribution before and after tackifying the EP granules are displayed in Fig. 14. The repose angles measured for the experimental heaps with uncoated and coated EP granules are 36.4° and 38.0°, respectively. The corresponding values obtained from DEM simulations are 36.0° and 37.6°, which cl osely match those of the experiment (Fig. 14 (A)). The values of the angle of repose show a negligible change as a result of coating of the minor component (EP) in both experiments and DEM simulations. In addition to comparing the angle of repose, the powder discharge time from the funnel can be affected by flowability of the powder mixture. It is observed that the total time taken

to empty the funnel changes from 2.22 s to 2.32 s when the EP granules are coated. This is about 5% increase in the discharge time, and indicates a slight decrease in flowability of the mixture with coated granules.

The spatial distribution pattern of the EP granules in the heap changes due to coating (Fig. 14 (B)); however, the rest of the particles, which are not coated, have the same pattern in all tests. For example, the CoV values for TAED particles before and after coating are 0.76 and 0.74, respectively, showing a negligible change. Also their spatial distribution patterns are very similar as displayed in Fig. 14 (C).

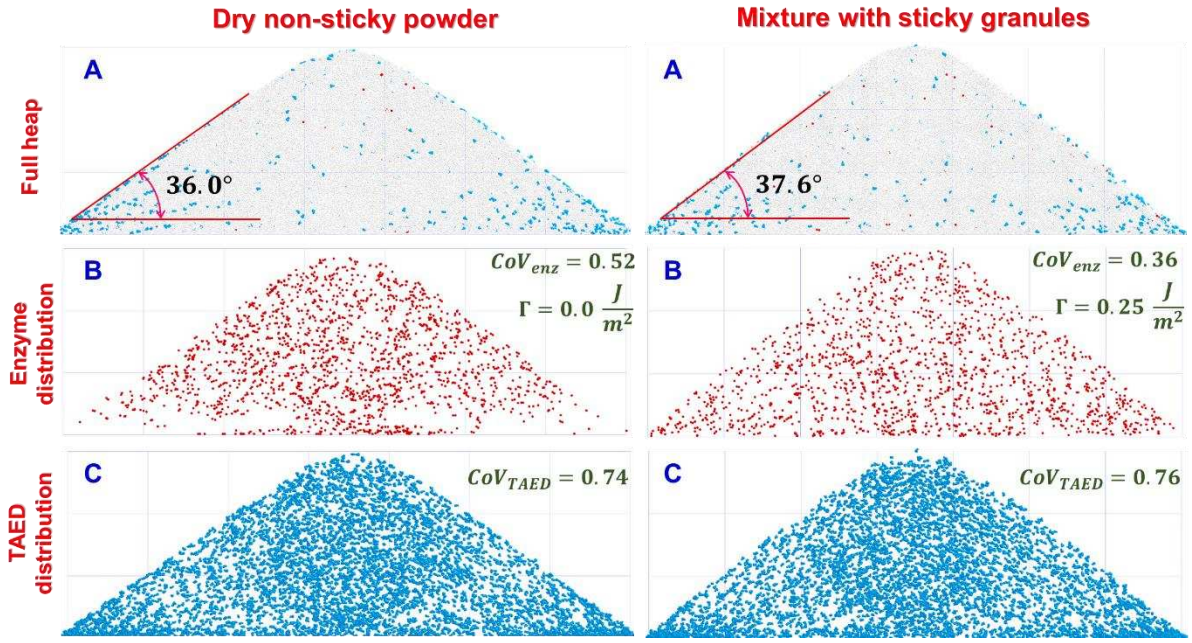

Fig. 14. Front view image of the simulated heap before and after coating, displaying the full spatial distribution of (A) all particles present, (B) the EP granules only (red), (C) the TEAD particles only (blue).

The Jenike flow function of the actual ternary mixture is also evaluated at different consolidation loads to assess the flowability of the mixture before and after coating as given in Fig. 15. The average value of ff_C has reduced from 6.3 to 4.4 due to the coating, indicating a reduction in flowability. Nevertheless, comparing the values of ff_C with those defining the classification of the flow regimes provided in Table 3 shows that the mixture remains in the easy-flowing regime for

different pre-consolidation stresses, even after coating the minor components. Also it is evident for both cases presented that the change in flow function as a function of pre-consolidation stress is insignificant. The EP granules are rounded in shape and act as rollers in the mixture during the shear test. In fact their spherical shape aids the whole mixture to flow more easily [59]. Conversely, when these rounded particles are made sticky, they function as “break” (damping effect) which partially deteriorates the flowability.

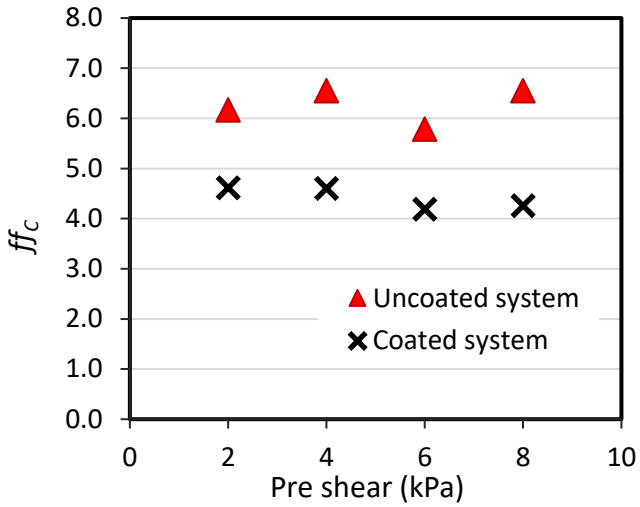

Fig. 15. Jenike flow function of the powder mixture before and after coating the EP granules.

3.4 Segregation mechanisms

The use of DEM gives an opportunity to have a closer look at the particles movement before and during the heap formation. To do so the mass fraction of the species after discharging from the funnel is calculated and plotted versus time to check if there is any pre-segregation occurring in the funnel. The formulation mass fractions of TAED and EP granules are about 0.06 and 0.02, respectively (Table 1). As shown in Fig. 16 the particles mass fraction starts from zero, then increases to a certain level, and continues with random fluctuations around their average mass fraction values over the discharge time towards the end. For the EP granules, there is no significant change in the average mass fraction through time which is an indication that the placebo granules do not pre-segregate in the funnel and the observed segregation is mainly due to the heap formation. For the TAED, a very slight decrease in its mass fraction occurs over the

discharge time mainly due to its larger size compared to the BP; nevertheless, this is not dominant comparing with the segregation taking place during the heap formation.

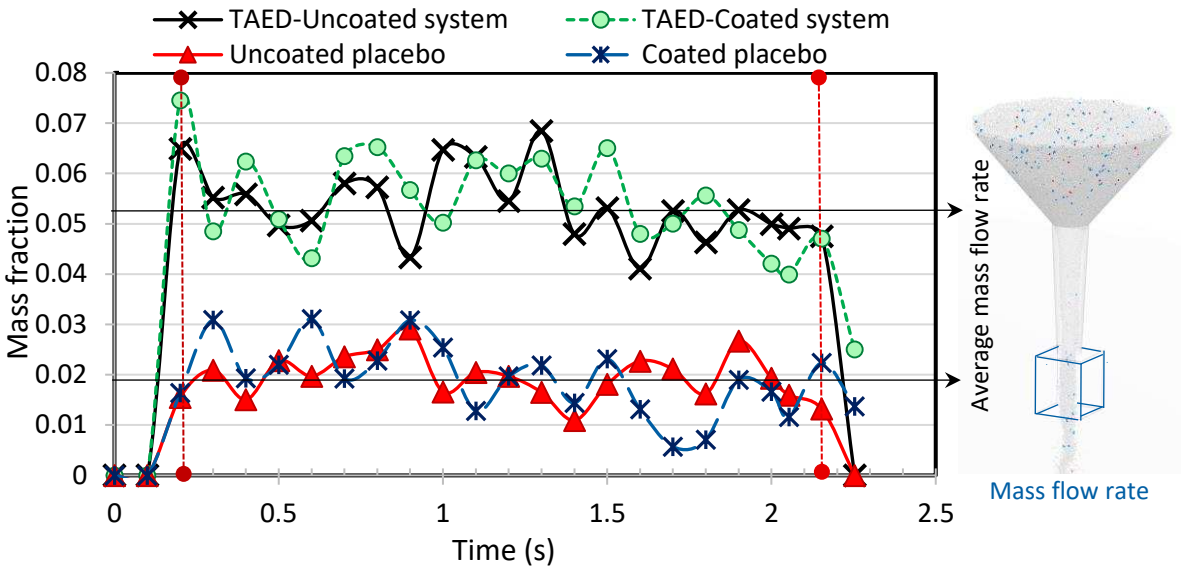

Fig. 16. The mass fraction variation of the EP and TAED particles versus the discharge time at the outlet of the funnel as given by DEM simulation.

Focusing on the heap formation process, the uncoated EP granules accumulate centrally with lower concentrations close to the side walls and the base as compared to the central region (Fig. 11). Their segregation in the centre is driven mainly by their high density, as otherwise, they would have segregated down to the heap corners because of their relatively large size compared to the main ingredient of the mixture (e.g. BP particles) as well as their rounded shape. To elucidate the underlying mechanisms of segregation, some EP granules are selected and followed during the heap formation as displayed in Fig. 17. As the dry uncoated EP granules fall down on the heap surface they push other particles away and get imbedded in a layer beneath the top moving layer (push-away effect [60]). In this case their rounded shape helps them to penetrate more deeply into the heap and escape from the shearing top layer. On the other hand, the coated granules show less penetration into the top layer (Fig. 17, t=1.74 s) and hence spread more over the heap surface compared with the uncoated ones. This is also observable from the top surface of the heap in the experiments (Fig. 18). The TAED particles, however, have much

less density and sphericity compared to the placebo granules, both of which prevent them from penetrating into the sublayers; thus they tumble down more freely and segregate to the corners. The penetration analysis indicates that the impact velocity of the particles changes the extent of segregation by affecting the level of penetration of the EP granules. Therefore, pouring the particles from a shorter height can potentially reduce the density-induced segregation.

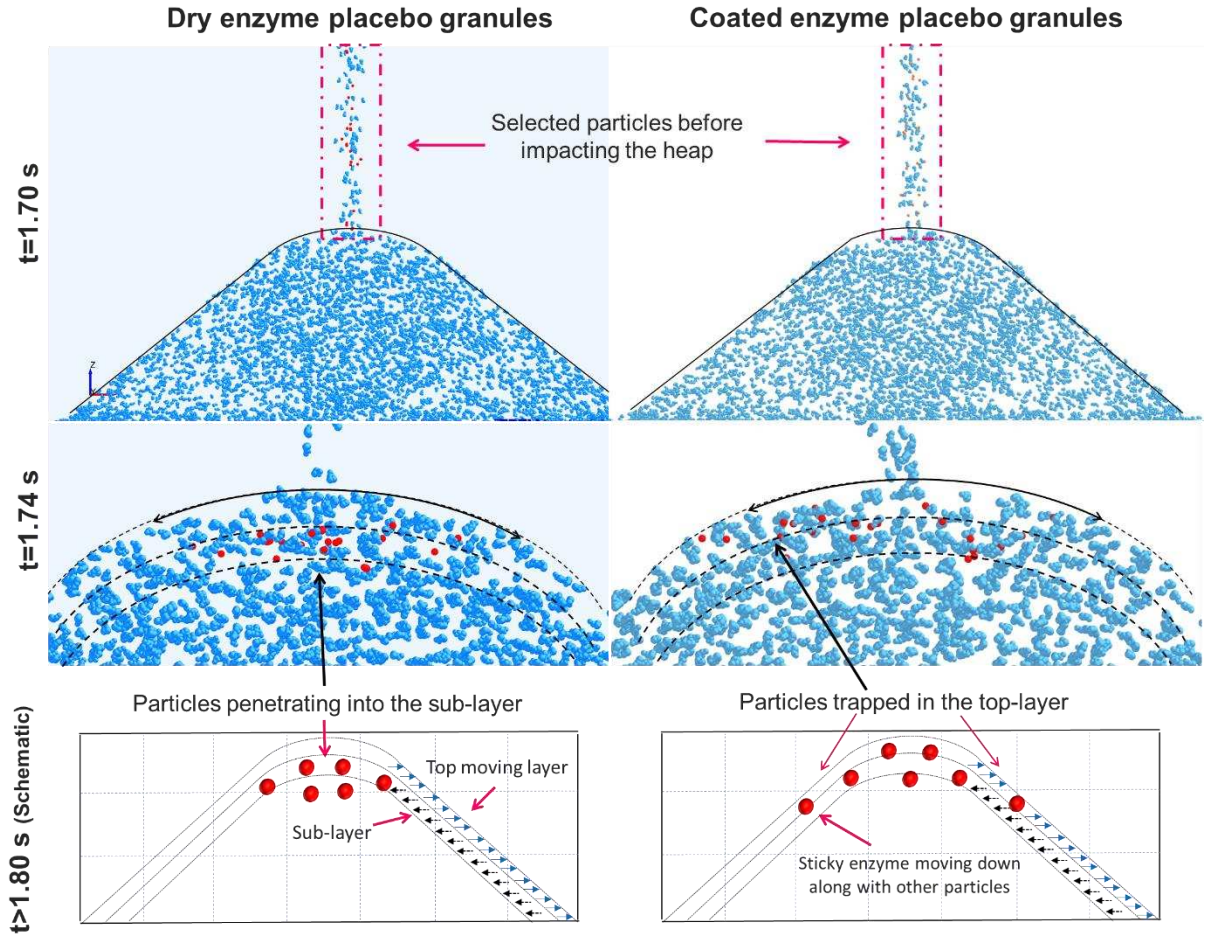

Fig. 17. The movement pattern of selected EP granules (red particles) immediately before and after falling on the heap surface (blue particles are TAED). A schematic of the enzyme movement is also displayed with size exaggeration.

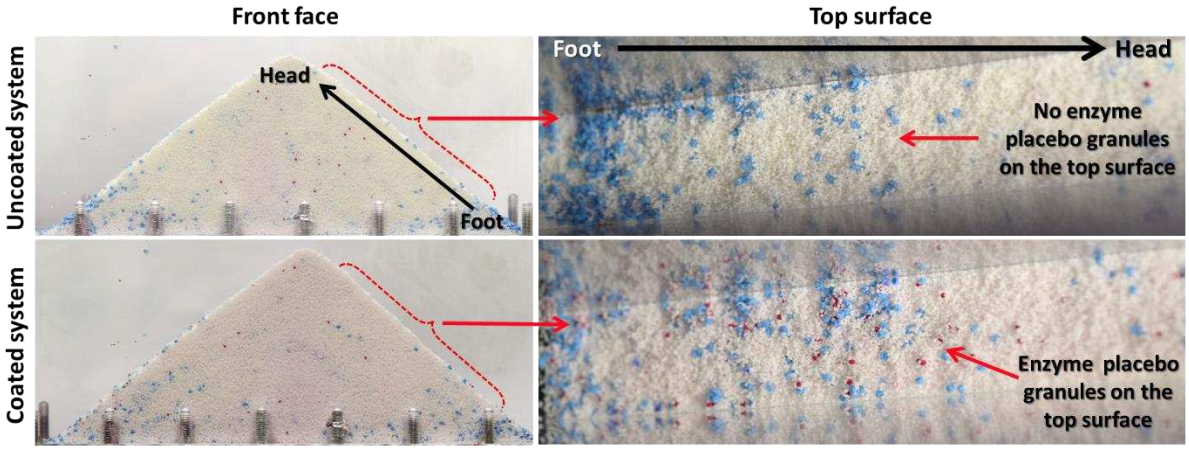

Fig. 18. The extent of penetration of uncoated and coated EP granules into the heap surface.

Coating the placebo granules attenuates the push-away mechanism using the damper-effect, i.e. any relative movement of the particles adjacent to the placebo granules will be damped because of the stickiness of the coated granules. In this case, as schematically illustrated in Fig. 17, the coated EP granules are mostly embedded in the top moving layer and follow the main stream of the mixture during the heap formation; therefore they reach the corners of the heap as well. This is clear from the analysis of the specific kinetic energy (kinetic energy per unit mass of the particle) of the granules during the heap formation, shown in Fig. 19, where the individual particles kinetic energy, as they first hit the heap surface, is plotted for the uncoated and coated cases. This graph shows that the granules specific kinetic energy drops dramatically following this event; nevertheless, a difference in the way the coated and uncoated granules behave is observed. The zoomed part of the graph shows that the specific kinetic energy of the dry placebo granules approaches zero very quickly and smoothly indicating that the particles stop their motion after the impact. For the coated particles, on the other hand, the kinetic energy stays non zero for a longer time showing that the particles maintain their motion for a longer time after hitting the heap surface. This corroborates the previous hypothesis made about the movement of sticky particles escorted by the rest of the particles on the top layer of the heap.

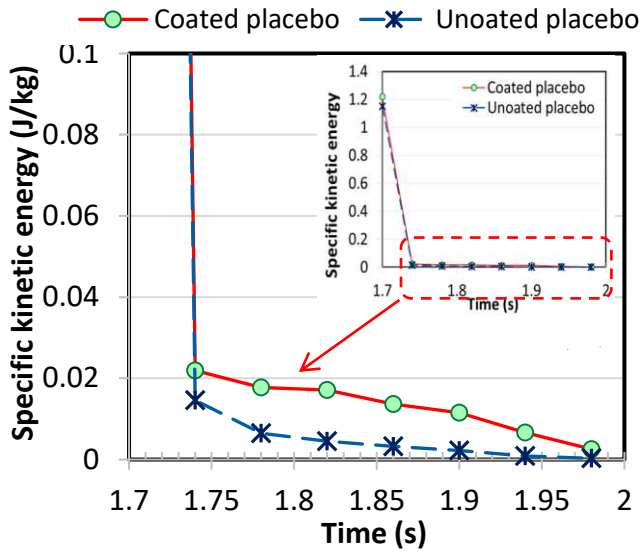

Fig. 19. The variation of specific kinetic energy of the selected EP granules versus time for a short period before and after hitting the heap surface.

3.5 Effect of coating level

The interfacial energy values utilised in the previous tests were scaled and tuned using the Cohesion number. In a case study, the interfacial energy values for all the particle contacts, i.e. the placebo-placebo, placebo-BP, and placebo-TAED interactions are set equal to 0.25 $\mathrm{J.m^{-2}}$ to see the effect of high interfacial energy on segregation. As displayed in Fig. 20 the EP granules accumulate in the corners and the segregation index in this case is 2.58 (CoV=0.98), which is even greater than the segregation index of the uncoated system. High interfacial energy between the placebo and BP particles causes the small BP particles to attach themselves to the EP granules. In this case, the EP granules act as seeds covered by BP small particles making large agglomerates. These agglomerates cannot penetrate into the sublayers of the heap, but rather avalanche down and promote the segregation (Fig. 20 (B)).

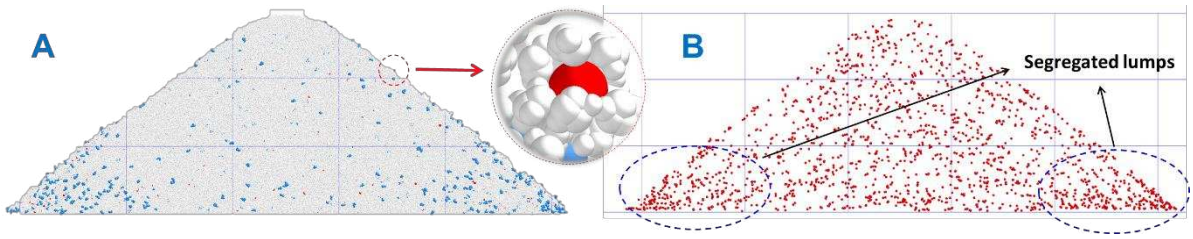

Fig. 20. The EP segregation after applying high interfacial energy values in DEM modelling. A) Presentation of all particles, B) presentation of EP granules only.

4 Conclusions

In this study, a systematic methodology is proposed for selection and calibration of the DEM input parameters with a particular focus on calibration of the particles interfacial energy with regards to their size, stiffness, shape, and density. As a proof of concept, this methodology is applied to modelling of segregation of low level ingredients in a ternary powder mixture. The particles are in different sizes, densities, shapes, and mass fractions based on a real model case of home washing powders. The segregating minor component (EP) is made sticky by coating it with a thin layer of PEG 400 and the rest of the species are unchanged. The interfacial energy values for the particles interaction are calibrated using experimental angle of repose and the dimensionless Cohesion number.

A good agreement between the experimental and DEM simulation results is observed. The experimental trends for the segregation tendency of the coated EP granules are replicated with high fidelity by DEM simulations. For the mixture with coated granules, the interfacial energies of the components are inferred by matching the experimental and simulated repose angles. The Cohesion number is used to scale the interfacial energy when reducing Young's modulus or changing the particle size for faster simulation. As a result, the segregation extent can be reliably predicted.

It is observed that before coating, the EP granules segregate to the central area of the heap due to their high density leaving the corners and side walls with a lower mass concentration. However, they are very well distributed over the entire heap after being coated. As a result, the segregation index value is reduced 40% in total and nearly 100% locally on the side walls. The rounded shape of the granules acts in favour of the push-away effect by which the EP granules penetrate more easily into the sublayers of the heap surface and segregate more.

It is also observed that coating minor ingredients does not change the flow properties of the mixture considerably and for the present case the mixture flowability remains in the easy flowing regime indicated by the flow function value (Jenike flow index). The DEM simulation results also show that in pseudo-2D systems, the segregation tendency is magnified on the walls while the middle layers of the heap are in a better condition. These trends can be readily predicted and observed by DEM simulation, considering the measured and calibrated particle properties such as shape, density, size, and surface adhesion.

5 Acknowledgments

This work is part of Chariot project, funded by the UK government's Advanced Manufacturing Supply Chain Initiative (AMSCI) [grant number 31587, 233189]. The authors are also grateful to Mrs Claire Duckitt, Mrs Clair Martin, the project manager, and Paul Gould as the overall coordinator of the project for their help.

References

[1] D.S. Nasato, C. Goniva, S. Pirker, C. Kloss, Coarse Graining for Large-scale DEM Simulations of Particle Flow – An Investigation on Contact and Cohesion Models, Procedia Engineering, 102 (2015) 1484-1490.

[2] J. Hærvig, U. Kleinhans, C. Wieland, H. Spliethoff, A.L. Jensen, K. Sørensen, T.J. Condra, On the adhesive JKR contact and rolling models for reduced particle stiffness discrete element simulations, Powder Technol, 319 (2017) 472-482.

[3] M.A. Behjani, N. Rahmanian, N. Fardina bt Abdul Ghani, A. Hassanpour, An investigation on process of seeded granulation in a continuous drum granulator using DEM, Adv Powder Technol, 28 (2017) 2456-2464.

[4] N. Jain, J.M. Ottino, R.M. Lueptow, Regimes of segregation and mixing in combined size and density granular systems: an experimental study, Granul Matter, 7 (2005) 69-81.

[5] H. Musha, G.R. Chandratilleke, S.L.I. Chan, J. Bridgwater, A.B. Yu, Effects of Size and Density Differences on Mixing of Binary Mixtures of Particles, Aip Conf Proc, 1542 (2013) 739-742.

[6] G.G. Pereira, N. Tran, P.W. Cleary, Segregation of combined size and density varying binary granular mixtures in a slowly rotating tumbler, Granul Matter, 16 (2014) 711-732.

[7] M. Asachi, A. Hassanpour, M. Ghadiri, A. Bayly, Analysis of Minor Component Segregation in Ternary Powder Mixtures, EPJ Web Conf., 140 (2017) 13013.

[8] I. Figueroa, H. Li, J. McCarthy, Predicting the impact of adhesive forces on particle mixing and segregation, Powder Technol, 195 (2009) 203-212.

[9] J. Yang, A. Silva, A. Banerjee, R.N. Dave, R. Pfeffer, Dry particle coating for improving the flowability of cohesive powders, Powder Technol, 158 (2005) 21-33.

[10] Q. Zhou, L. Qu, I. Larson, P.J. Stewart, D.A.V. Morton, Effect of mechanical dry particle coating on the improvement of powder flowability for lactose monohydrate: A model cohesive pharmaceutical powder, Powder Technol, 207 (2011) 414-421.

[11] A. Samadani, A. Kudrolli, Segregation Transitions in Wet Granular Matter, Phys Rev Lett, 85 (2000) 5102-5105.

[12] F. Fulchini, U. Zafar, C. Hare, M. Ghadiri, H. Tantawy, H. Ahmadian, M. Poletto, Relationship between surface area coverage of flow-aids and flowability of cohesive particles, Powder Technol, 322 (2017) 417-427.

[13] J.J. McCarthy, Turning the corner in segregation, Powder Technol, 192 (2009) 137-142.

[14] E.H.J. Kim, X.D. Chen, D. Pearce, Effect of surface composition on the flowability of industrial spray-dried dairy powders, Colloids and Surfaces B: Biointerfaces, 46 (2005) 182-187.

[15] A.-S. Persson, G. Alderborn, G. Frenning, Flowability of surface modified pharmaceutical granules: A comparative experimental and numerical study, Eur J Pharm Sci, 42 (2011) 199-209.

[16] A. Spillmann, A. Sonnenfeld, P. Rudolf von Rohr, Effect of surface free energy on the flowability of lactose powder treated by PECVD, Plasma Processes and Polymers, 5 (2008) 753-758.

[17] J.J. Nijdam, T.A.G. Langrish, The effect of surface composition on the functional properties of milk powders, J Food Eng, 77 (2006) 919-925.

[18] H. Li, J.J. McCarthy, Controlling Cohesive Particle Mixing and Segregation, Phys Rev Lett, 90 (2003) 184301.

[19] P. Begat, D.A.V. Morton, J.N. Staniforth, R. Price, The Cohesive-Adhesive Balances in Dry Powder Inhaler Formulations I: Direct Quantification by Atomic Force Microscopy, Pharmaceutical Research, 21 (2004) 1591-1597.

[20] A. Hassanpour, M. Eggert, M. Ghadiri, Analysis of segregation of binary mixtures of particulate solids due to size, density and cohesion, The 6th International Conference on Micro-mechanics of Granular Media, Powders and Grains 2009Golden Colorado, USA, 2009, pp. 687-690.

[21] K.L. Johnson, K. Kendall, A.D. Roberts, Surface Energy and the Contact of Elastic Solids, Proceedings of the Royal Society of London A: Mathematical, Physical and Engineering Sciences, 324 (1971) 301-313.

[22] B.V. Derjaguin, V.M. Muller, Y.P. Toporov, Effect of contact deformations on the adhesion of particles, J Colloid Interf Sci, 53 (1975) 314-326.

[23] M. Pasha, S. Dogbe, C. Hare, A. Hassanpour, M. Ghadiri, A linear model of elasto-plastic and adhesive contact deformation, Granul Matter, 16 (2014) 151-162.

[24] C. Thornton, Z. Ning, A theoretical model for the stick/bounce behaviour of adhesive, elastic-plastic spheres, Powder Technol, 99 (1998) 154-162.

[25] D. Tabor, Surface forces and surface interactions, J Colloid Interf Sci, 58 (1977) 2-13.

[26] H. Hertz, Ueber die Berührung fester elastischer Körper (on the contact of elastic solids), Journal für die reine und angewandte Mathematik (Crelle's Journal), 1882, pp. 156–171.

[27] H. Deresiewicz, R.D. Mindlin, U. Columbia, E. Department of Civil, Elastic spheres in contact under varying oblique forces, 1952.

[28] A. Di Renzo, F.P. Di Maio, Comparison of contact-force models for the simulation of collisions in DEM-based granular flow codes, Chemical Engineering Science, 59 (2004) 525-541.

[29] M.M. Martín, Introduction to software for chemical engineers, CRC Press2014.

[30] W.H. Hager, Wilfrid Noel Bond and the Bond number, J Hydraul Res, 50 (2012) 3-9.

[31] M. Alizadeh Behjani, A. Hassanpour, M. Ghadiri, A. Bayly, Numerical Analysis of the Effect of Particle Shape and Adhesion on the Segregation of Powder Mixtures, EPJ Web Conf., 140 (2017) 06024.

[32] J.F. Favier, M.H. Abbaspour-Fard, M. Kremmer, A.O. Raji, Shape representation of axi-symmetrical, non-spherical particles in discrete element simulation using multi-element model particles, Engineering Computations (Swansea, Wales), 16 (1999) 467-480.

[33] M. Alizadeh, A. Hassanpour, M. Pasha, M. Ghadiri, A. Bayly, The effect of particle shape on predicted segregation in binary powder mixtures, Powder Technol, 319 (2017) 313-322.

[34] M. Price, V. Murariu, G. Morrison, Sphere clump generation and trajectory comparison for real particles, Proceedings of Discrete Element Modelling 2007, (2007).

[35] A. Hassanpour, M. Pasha, L. Susana, N. Rahmanian, A.C. Santomaso, M. Ghadiri, Analysis of seeded granulation in high shear granulators by discrete element method, Powder Technol, 238 (2013) 50-55.

[36] W.N. Bond, The surface tension of a moving water sheet, Proceedings of the Physical Society, 47 (1935) 549.

[37] S.C. Thakur, J.Y. Ooi, H. Ahmadian, Scaling of discrete element model parameters for cohesionless and cohesive solid, Powder Technol, 293 (2016) 130-137.

[38] R. Moreno-Atanasio, B.H. Xu, M. Ghadiri, Computer simulation of the effect of contact stiffness and adhesion on the fluidization behaviour of powders, Chemical Engineering Science, 62 (2007) 184-194.

[39] H. Ahmadian, Analysis of enzyme dust formation in detergent manufacturing plant, Institute of Particle Science and Engineering, University of Leeds, United Kingdom, 2009.

[40] K. Van Ness, Surface tension and surface entropy for polymer liquids, Polymer Engineering & Science, 32 (1992) 122-129.

[41] C.J. van Oss, M.K. Chaudhury, R.J. Good, Monopolar surfaces, Adv Colloid Interfac, 28 (1987) 35-64.

[42] H.J. Butt, M. Kappl, Surface and Interfacial Forces, Wiley2009.

[43] L.T. Fan, R.H. Wang, On mixing indices, Powder Technol, 11 (1975) 27-32.

[44] D.K. Rollins, D.L. Faust, D.L. Jabas, A superior approach to indices in determining mixture segregation, Powder Technol, 84 (1995) 277-282.

[45] R. Hogg, Characterization of relative homogeneity in particulate mixtures, Int J Miner Process, 72 (2003) 477-487.

[46] S.-H. Chou, Y.-L. Song, S.-S. Hsiau, A Study of the Mixing Index in Solid Particles, Kona Powder Part J, (2016) 2017018.

[47] B.N. Asmar, P.A. Langston, A.J. Matchett, A generalised mixing index in distinct element method simulation of vibrated particulate beds, Granul Matter, 4 (2002) 129-138.

[48] G.R. Chandratilleke, A.B. Yu, J. Bridgwater, K. Shinohara, A particle-scale index in the quantification of mixing of particles, Aiche J, 58 (2012) 1099-1118.

[49] P.M.C. Lacey, The mixing of solid particles, Chemical Engineering Research and Design, 75 (1997) S49-S55.

[50] A. Kukukova, J. Aubin, S.M. Kresta, A new definition of mixing and segregation: Three dimensions of a key process variable, Chemical Engineering Research and Design, 87 (2009) 633-647.

[51] A. Kukuková, B. Noël, S.M. Kresta, J. Aubin, Impact of sampling method and scale on the measurement of mixing and the coefficient of variance, Aiche J, 54 (2008) 3068-3083.

[52] L.T. Fan, J.R. Too, R.M. Rubison, F.S. Lai, Studies on multicomponent solids mixing and mixtures Part III. Mixing indices, Powder Technol, 24 (1979) 73-89.

[53] M.J. Rhodes, Introduction to particle technology, John Wiley & Sons2008.

[54] G.Y. Onoda, E.G. Liniger, Random loose packings of uniform spheres and the dilatancy onset, Phys Rev Lett, 64 (1990) 2727-2730.

[55] K.R. Poole, R.F. Taylor, G.P. Wall, Mixing Powders to Fine-scale Homogeneity: Studies of Batch Mixing, UK Atomic Energy Authority Research Group1964.

[56] A.W. Jenike, Storage and flow of solids, Bulletin 123, Utah Engineering Experiment Station, University of Utah, Salt Lake City, Utah, 1964.

[57] J. Seville, C.-Y. Wu, Chapter 2 - Bulk Solid Characterization, Particle Technology and Engineering, Butterworth-Heinemann, Oxford, 2016, pp. 17-38.

[58] J. Schwedes, Review on testers for measuring flow properties of bulk solids, Granul Matter, 5 (2003) 1-43.

[59] X. Fu, D. Huck, L. Makein, B. Armstrong, U. Willen, T. Freeman, Effect of particle shape and size on flow properties of lactose powders, Particuology, 10 (2012) 203-208.

[60] G. Félix, N. Thomas, Evidence of two effects in the size segregation process in dry granular media, Phys Rev E, 70 (2004) 051307.